

PalArch's Journal of Archaeology of Egypt / Egyptology

EFFECT OF RESTITUTION COEFFICIENT IN CFD SIMULATION OF SOLID-LIQUID TAPERED INVERSE FLUIDIZED-BED HYDRODYNAMICS

*H. Upender*¹, *K. Anand Kishore*², *T.Srinivas*³, *S.Mishara*⁴, *P.Suresh Kumar*⁵

¹ Department of chemical engineering, National Institute of Technology Warangal, Telangana, India-506004,

² Al Imam Islam University, Alfalah - Riyadh- Saudi Arabia -13314,

³ Department of Chemical and Petroleum Engineering, UIE, Chandigarh University, Gharuan. Mohali, India-140413,

⁴ University of Petroleum and Energy studies- Dept of Mechanical, Engineering,

⁵ University of Petroleum and Energy studies- Dept of Electrical and Electronics Engineering

Email: ¹ upender07053@gmail.com

H. Upender, K. Anand Kishore, T.Srinivas, S.Mishara, P.Suresh Kumar: Effect of restitution coefficient in CFD simulation of solid-liquid tapered inverse fluidized-bed hydrodynamics -- PalArch's Journal Of Archaeology Of Egypt/Egyptology 17(9). ISSN 1567-214x

Keywords: Coefficient of restitution; Liquid-solid; Tapered inverse fluidized bed; Computational fluid dynamics; Hydrodynamic.

ABSTRACT

In the present work, an investigation made to develop a solid-liquid tapered inverse fluidized bed reactor (TIFBR). It essentially deals with the simulation of a TIFBR in computational fluid dynamics (CFD) using the software Ansys Fluent v17. In the present investigation, to analyze the effect of the elasticity of particle collision on the hydrodynamic characteristics of a TIFBR patched with 895 kg/m³ particles. The simulation is conducted using the Eulerian multifluid model, which is combined with the solid particle kinetic theory. The coefficients of exchange are determined by applied the Gidaspow drag function. The numerical findings were confirmed with experimental data (bed height and Voidage) and demonstrated that the model is capable of predicting the hydrodynamics of TIFBR. To determine the impact of the elasticity of solids collision, various estimated values of the restitution coefficient (RC) (0.85 to 1.0) were used in the numerical and their results were observed in detail. Simulations were done

for two various solid-phase wall boundary (0.5&1.0) conditions. Bubble development was not found for perfectly elastic collision. The evolution of the bubble started when the restitution coefficient was set below 1.0, and the space occupied by the bubbles in the bed grown with a decrease in the restitution coefficient.

1. Introduction

The inverse fluidized bed is having the wide range of applications in sugar industries, wastewater treatment, and power industries, oil, medical, agricultural due to their good mixing and the higher rate of heat and mass transfer [1]. Even though, at the point when the compactness of solids lower than that of liquid, the proper fluidized bed has been also used intended fluidized bed suitable for inverse fluidization. To overcome the problems like high energy requirement, power consumption, time consumption, and to get the high rate of heat and mass transfer, referred as the inverse fluidization method. In biotechnology and synergist substance response designing, the inverse fluidization has been developed for enhanced selectivity and yield. In these, lower density solids are fluidized by the downward flow of liquid moreover fluidization can be achieved in the downward [2]. In during inverse fluidization processes, three methods, to be specified those are batch, semi and fully fluidization. The examination concerns the task goes from a condition of batch state to a condition of the completely fluidized bed. Low thickness particles ($<534 \text{ kg/m}^3$) which improve the framework [3]. The downwards flow fluidization phenomenon suitable to the recuperation of over-covered particles at the base of the bed. In addition, the fluid and the biogas stream in countercurrent bearings, which enhances bed expansion and high rate of heat and mass transfer [4]. In wastewater treatment by using the inverse fluidization processes the hydraulic retention time is effecting factor on the processes [8]. The heat and mass transfer coefficient can also found in three-phase inverse fluidization [9]. The Bed porosity will be also affected by water treatment [4]. Generally, in two-phase inverse fluidization processes, the particles have the lower density than the water and the fluidization is in downward flow in this way the buoyancy force is acting against the continuous downward flow of liquid. In three phases inverse fluidization, we can send the gas countercurrent to the liquid phase. We can also predict the minimum fluidization velocity correlations in three phases and two phases by using experimental data in the inverse fluidization [5]. The benefits of inverse fluidization are productive control of biofilm thickness, expanded mass exchange rate and simplicity of re-fluidization. In perspective of these interesting favorable circumstances, inverse fluidized bed (IFB) is connected to handle the effluent from residential and process (Fan, 1989, Calderon et al., 1998). In process of CFD simulation of liquid–solid multiphase stream, the Euler–Euler two-liquid model is applied. This is perhaps because of its compromise among computational cost, level of detailed characteristics provided, and capability of applicability. Within the bounds of Euler–Euler

approach, fluid, and solid phases are dealt with scientifically as interpenetrating times. Coupling is accomplished through the interface forces containing the lift force, drag force and essential mass force. In the Euler– Euler model, the solid phase is viewed as a continuum, and hence, solid phase pressure and viscosity are expected to be demonstrating[6]. The Kinetic Granular Flow Theory (KTGF) has been generally accepted as an integral constitutive model for simulating the solid's flow properties. This is absolutely the element to be considered. In two previous cases, the great understanding was asserted amongst expectations and exploratory outcomes, though the CFD demonstrate in the third case neglected to anticipate a high-shallow speed stream progress. Fluid converse fluidized beds should, at any rate on a fundamental level, be less complex to display than gas-fluidized beds, since the hydraulics exist more analogous, agitation is significantly below of a influence and the, confuse among the stage compactness is lessened. Between molecule, crashes are additionally extraordinarily lessened, or even truant (Gidaspow and Lu, 1998) because of the fluid film isolating grains as they come close each other. Besides, a portion of the components which usually confound genuine gas-conventional beds, for example, non-round molecule wide and shape molecule estimate dispersions, have a tendency to be lessened or truant in fluid fluidized beds, these regularly being made out of mono-sized glass globules fluidized by water[7]. In hydrodynamics studies, the minimum fluidization velocity will be increased by increasing particle diameter[10].

The aim of the current work is to investigate the function of elasticity of solids collisions in simulating the hydrodynamics of a TIFBR patched with lower density solids. In order to decide the function of the elasticity of the particle collision, conceivable estimations of the coefficient of restitution have been used in the simulation. The simulations were carried out under two varies solid-phase wall boundary conditions for all the estimations of coefficient of restitutions. The impact on granular temperature, solids velocity and volume fraction were determined by comparing the outcomes for various estimations of the coefficient of restitution. The Simulation data were also compared with experimental data in order to achieve the optimal estimate of the restitution coefficient.

2. Nomenclature:

Notation	Description	Units
Re	Reynolds no	Dimensionless
g	Gravitational force	ms ⁻²
e _{sw}	Restitution coefficient	-
e _{ss}	-	-
g ₀	radial distribution coefficient,	Dimensionless

K	interphase exchange coefficient,	Dimensionless
t	time	s
C_D	Drag coefficient	Dimensionless
$k_{\Theta s}$	diffusion coefficient for granular energy,	Dimensionless
d	Diameter	m
Greek letters		
ϵ	Volume fraction	Dimension less
η	dynamic viscosity,	Pa. s
λ	bulk viscosity	Pa. s
$\gamma_{\Theta s}$	collision dissipation of energy,	$\text{kg/s}^3 \cdot \text{m}$
μ	Viscosity	Pa. s
v	Velocity	m/s
ρ	Density	Kg/m^3
Φ	An angle of internal friction	deg
Φ	a transfer rate of kinetic energy,	$\text{kg/s}^3 \text{ m}$
$\bar{\tau}$	stress tensor,	Pa
\bar{l}	stress tensor,	Dimensionless

3. Materials and methods

2.1 Experimental Setup:

In the CFD simulation the empirical drag laws are applied to measure the momentum exchange between the solid and fluid phase. It gives correct and quick information about various parameters. The advances in innovation require more extensive and more itemized data about the stream inside an involved zone, and CFD meets this objective superior to some other strategy, (i.e., theoretical or experimental methods). The numerical plans and techniques

whereupon CFD are based are enhancing quickly, so CFD results are progressively reliable. CFD is a dependable tool for design and analyses.

In the present work of tapered inverse fluidization, the liquid was tap water is used as liquid media and the polymer of the low-density material of 0.03m diameter is used as solid media, the acrylic column is tapered and has a 0.07m top and 0.25m bottom diameter and height is 0.58m. The stream of the liquid (water) through this opening was controlled by the use of valves. Water pumped through a pipe which associated with manometer which is loaded with mercury by 0.5HP engine pump to the highest point of the segment the setup shown in Fig. 1.

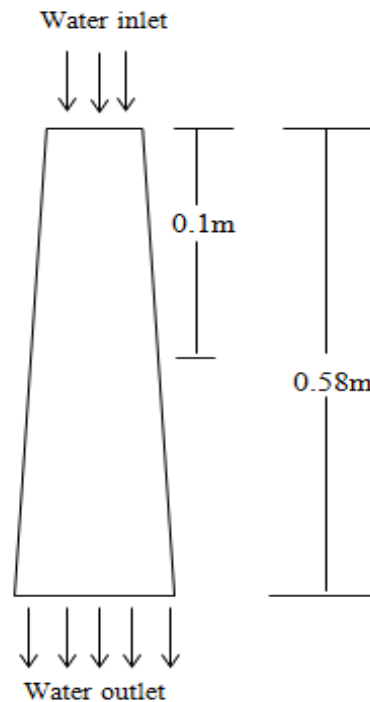


Fig.1 Schematic of inverse fluidized bed

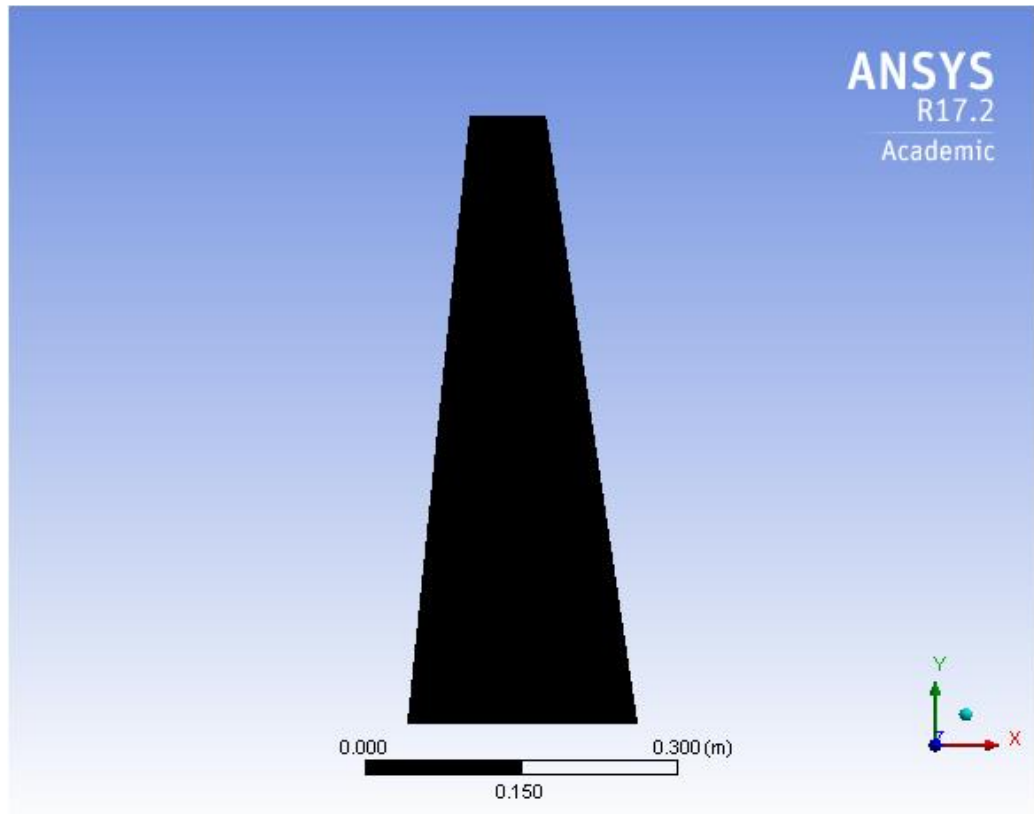


Fig.2 Schematic mesh of Inverse fluidized bed

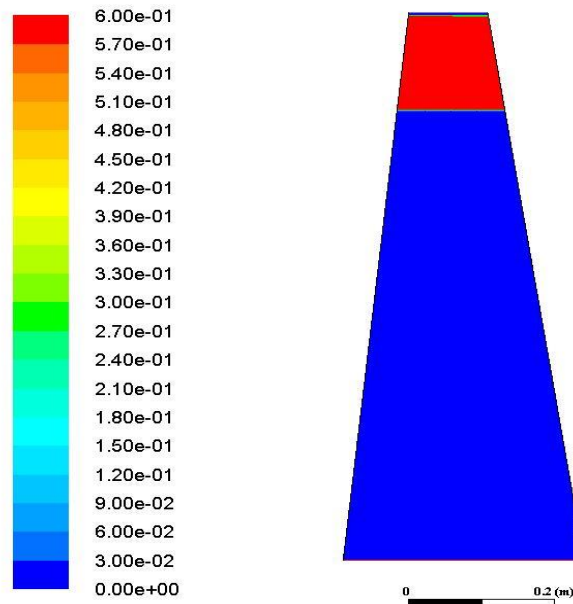


Fig.3 Computational domain with the boundary conditions

2.2 Numerical Simulation

Table 1 Parameters used in simulations:

Parameters	Numerical value	Units
Reactor size	0.07*0.25*0.58	m
Grid number	50*600	-
Convergence criteria	10 ⁻³	s
Maximum iterations	10000	s
Time step size	0.01	s
Discretization method	First order upwind scheme	-
Model precision	Double	-
Initial volume fraction(solid)	0.6	-
e_{sw}	0.9	-
Operating pressure	1.013 × 10 ⁵	Pa
Granular viscosity	Gidaspow (1994)	Pas
Granular bulk viscosity	Lun et al. (1984)	Pas
Solid pressure	Lun et al. (1984)	Pa
Radial distribution	Lun et al. (1984)	-
Drag model	Gidaspow	-
e_{ss} (Restitution coefficient)	0.85,0.9,0.95,0.99,1	-
Φ (specularity coefficient)	0.5&1.0	-
Velocity(liquid)	(0.14-0.1.35)	m/s
Particle diameter	0.03	m
Density of particle (ρ_s)	930	Kg/m ³
Density of water(ρ_l)	1000	Kg/m ³
Initial bed height	0.1	m

Simulation model

All simulations were done using 2D model in view of the experiment as shown from Fig. 2 and Fig 3. The setup top was 0.075 m, bottom was 0.25m and the tallness was 0.58 m. The initial bed of solids at the top of the bed was packed with 0.03 m and the density was 930 kg/m³.and liquid sent with the constant speed of 0.14m/s from the top section of the reactor.

Conditions for monitoring

The Euler– Euler two-liquid model was used to determine the hydrokinetics of liquid– solids system in the reverse tapered bed. Conservation of mass and momentum governing equations provide for the interpenetrating liquid and solid phases.

Simulation model parameters are tabulated in Table.1

$$\partial/\partial t(\epsilon_1 \rho_1) + \nabla \cdot (\epsilon_1 \rho_1 \vec{v}_l) = 0 \tag{1}$$

$$\partial/\partial t(\epsilon_s \rho_s) + \nabla \cdot (\epsilon_s \rho_s \vec{v}_s) = 0 \tag{2}$$

$$\begin{aligned} \partial/\partial t(\epsilon_1 \rho_1 \vec{v}_l) + \nabla \cdot (\epsilon_1 \rho_1 \vec{v}_l \vec{v}_l) \\ = -\epsilon_1 \nabla p + \nabla \cdot \bar{\tau}_l + \epsilon_1 \rho_1 \mathbf{g} + K_{sl}(\vec{v}_s - \vec{v}_l) \end{aligned} \tag{3}$$

$$\begin{aligned} \bar{\tau}_l \\ = \epsilon_l \mu_l (\nabla \vec{v}_l + \nabla \vec{v}_l^T) \\ - \frac{2\alpha_l \mu_l}{3} (\nabla \cdot \vec{v}_l) \bar{I} \end{aligned} \tag{4}$$

$$\partial/\partial t(\epsilon_s \rho_s \vec{v}_s) + \nabla \cdot (\epsilon_s \rho_s \vec{v}_s \vec{v}_s) = -\epsilon_s \nabla p - \nabla \cdot \bar{\tau}_s + \epsilon_s \rho_s \mathbf{g} + K_{sl}(\vec{v}_l - \vec{v}_s) \tag{5}$$

$$\begin{aligned} \bar{\tau}_s = \epsilon_s \mu_s (\nabla \vec{v}_s + \nabla \vec{v}_s^T) - \epsilon_s \left(\lambda_s - \frac{2}{3} \mu_s \right) (\nabla \cdot \vec{v}_s) \bar{I}, \end{aligned} \tag{6}$$

$$\begin{aligned} \frac{3}{2} \left[\frac{\partial}{\partial t} (\epsilon_s \rho_s \theta_s) + \nabla \cdot (\epsilon_s \rho_s \vec{v}_s \theta_s) \right] \\ = (-\rho_s \bar{I} + \bar{\tau}_s) : \nabla \vec{v}_s + \nabla \cdot (k_{\theta_s} \nabla \theta_s) - \gamma \theta_s + \theta_{sl} \end{aligned} \tag{7}$$

$$\lambda_s = \frac{4}{3} \epsilon_s \rho_s d_s g_{o,ss} (1 + e_{ss}) \left(\frac{\theta_s}{\pi} \right)^{1/2} \tag{8}$$

$$\begin{aligned} \rho_s \\ = \epsilon_s \rho_s \theta_s \\ + 2\rho_s (1 + e_{ss}) \epsilon_s^2 g_{o,ss} \theta_s \end{aligned} \tag{9}$$

$$\begin{aligned} \mu_s = \frac{4}{5} \epsilon_s^2 \rho_s d_s g_{o,ss} (1 + e_{ss}) \left(\frac{\theta_s}{\pi} \right)^{\frac{1}{2}} + \frac{\epsilon_s \rho_s d_s \sqrt{\theta_s \pi}}{6(3 - e_{ss})} \\ * \left[1 + \frac{2}{5} (1 + e_{ss}) (3e_{ss} - 1) \epsilon_s g_{o,ss} \right] \end{aligned} \tag{10}$$

$$g_{o,ss} = \left[1 - \left(\frac{\epsilon_s}{\epsilon_{s,max}} \right)^{\frac{1}{3}} \right]^{-1} \tag{11}$$

$$K_{sl} = \frac{3}{4} C_D \frac{\epsilon_s \epsilon_l \rho_1 (\vec{v}_s - \vec{v}_l)}{d_s} \epsilon_l^{-2.65} \text{For } \epsilon_l > \tag{12}$$

$$K_{sl} = 150 \frac{\epsilon_s (1 - \epsilon_l) \mu_l}{\epsilon_l d_s^2} + 1.75 \epsilon_s \rho_1 \frac{(\vec{v}_s - \vec{v}_l)}{d_s} \text{For } \epsilon_l \leq \tag{13}$$

0.8

With

$$C_D = \frac{24}{\epsilon_l Re_s} [1 + 0.15 (\epsilon_l Re_s)^{0.687}] \text{For } Re_s \leq 1000 \tag{14}$$

For $Re_s > 1000$

$$Re_s = \rho_1 d_s \frac{|\vec{v}_s - \vec{v}_l|}{\mu_l} \tag{15}$$

Where Re is the Reynolds noand C_D is the drag coefficient.

4. Results and discussion

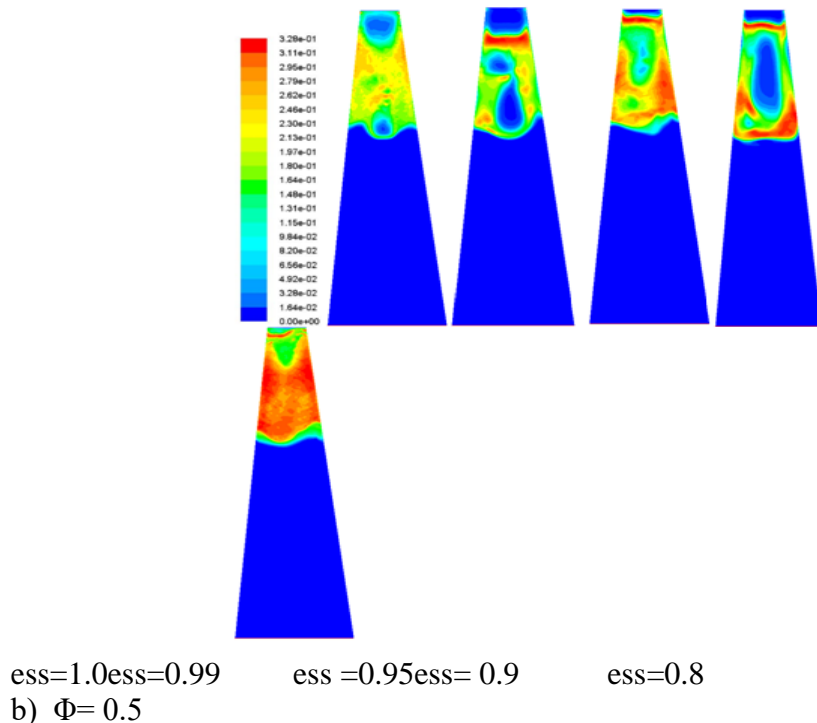
In the present work we have to investigate about the impact of the particle-particle coefficient of compensation by changing the different drag between

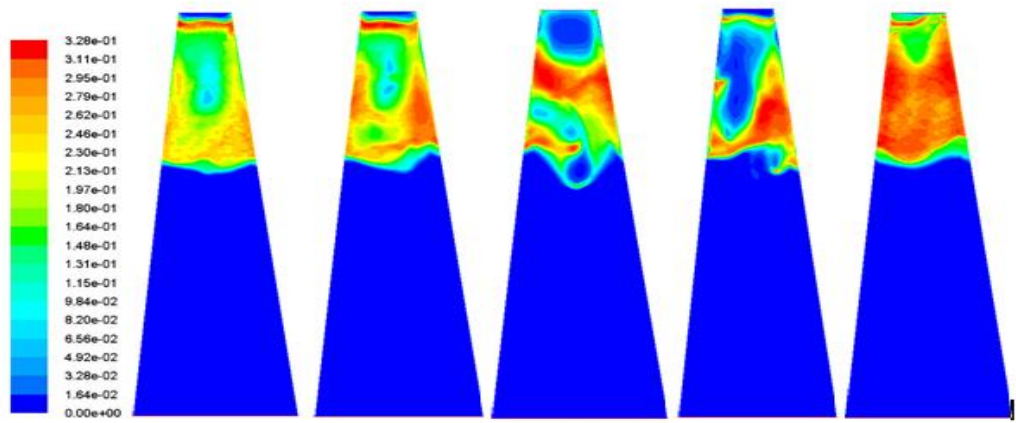
solid-wall on the Euler–Euler CFD simulation of percolating tapered inverse fluidized-bed hydrokinetics without varying alternate parameters in the reenactment. And we have compared bed height, Voidage experimental results with simulated results.

4.1. Impact of the coefficient of compensation

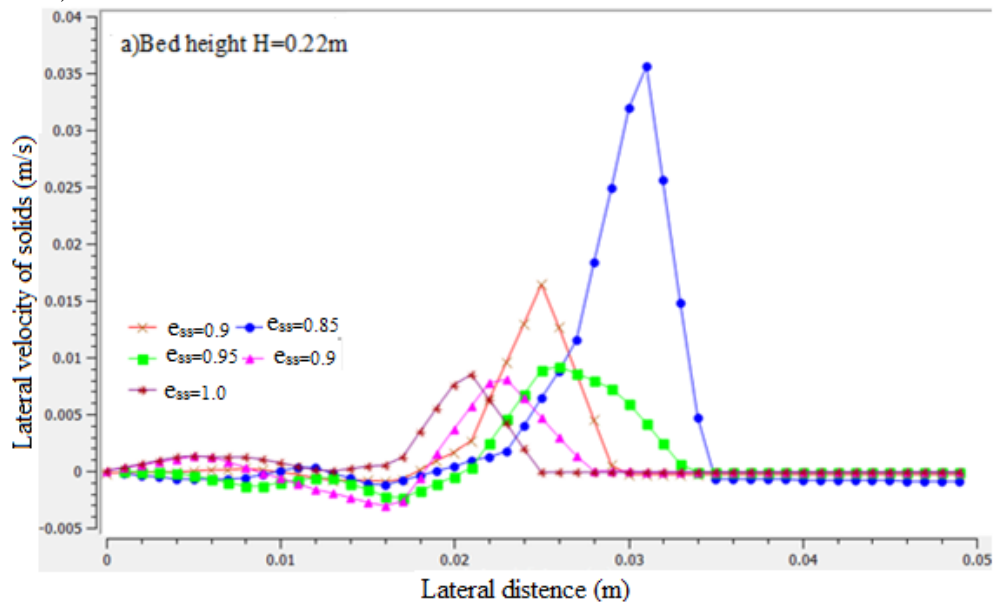
Five unique estimations concerned coefficient of restitution ($ess = 1.0, 0.99, 0.95, 0.90$ and 0.85) were used. A lower estimation of ess suggested much loss of energy anticipated to particle– fluid collisions. It was watched that simulation comes about were delicate to ess . The fact that the Euler– Euler two-liquid model used solid phase properties (solid mass consistency, solid weight, and solid shear thickness). Which elements of ess , in the figuring of the solid force. The prompt molecule fixation dispersions inside the bed for the various estimations concerned coefficient of compensation are premeditated in Fig. 4. Different conditions were accounted for two varies solid phase wall boundary conditions, those are the no-slip ($\phi = 1.0$) and partial-slip ($\phi = 0.5$) conditions in Fig. 4 and all through the bed was seen at $ess = 0.95$, For $ess = 0.99$, the most extreme molecule volume fraction with smooth inverse fluidized bed stature was watched, which showed the decent quality in the reactor. It was additionally watched that there exist no deliberate contrast among the outcomes for the no-slip state ($\phi = 1.0$) and the halfway slip state ($\phi = 0.5$) but in no-slip condition solids volume fraction high when compare partial slip condition.

$\Phi=1.0$





$e_{ss}=1.0$ $e_{ss}=0.99$ $e_{ss}=0.95$ $e_{ss}=0.9$ $e_{ss}=0.85$
Fig.4. Flow profile transformations as restitution coefficient variations, colored according to the solids volume fraction for varies Specularity coefficients: a) 1.0 and b) 0.5



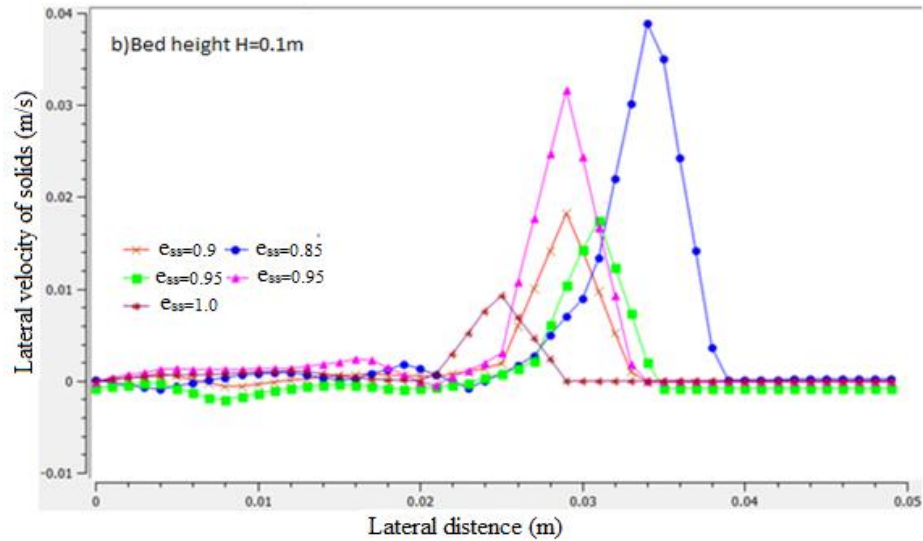
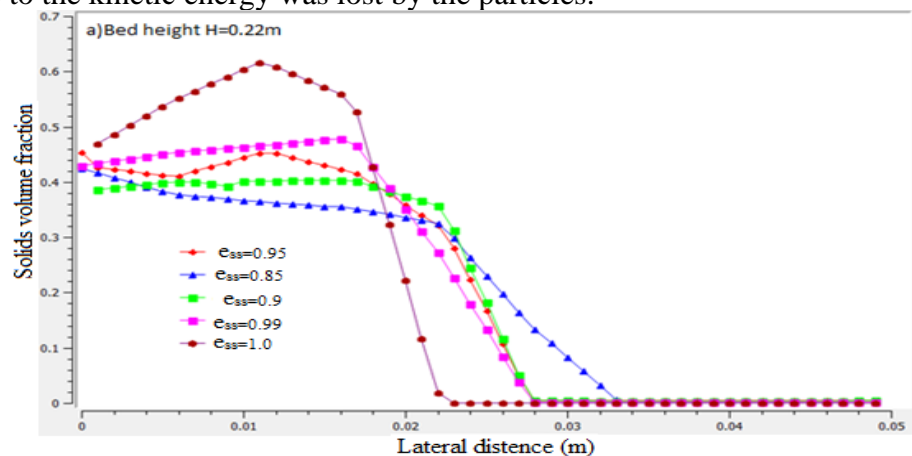


Fig .5 Lateral velocity profiles of solids along the lateral direction for varies restitution coefficients at different bed heights a) 0.22m and b)0.1m

From fig 5. We were observed that from the reproduction comes about the lateral velocity of solid particles along the lateral distance in the tapered opposite fluidized bed. will be certain in the right hand side of the positive and negative in left hand side of the hub, by expanding the restitution coefficient ($e_{ss} = 0.85$ to $e_{ss}=1.0$) communication between the solid speed of particles development expanded at $e_{ss}=0.99$ & $e_{ss}=0.9$ other than at outstanding restitution coefficients relatively same and the speed of particles at center of the bed was high and at walls of the fluidized bed the velocity was zero.

At various bed heights from the channel, the speed of solids was expanded the bed height at $H=0.22m$ the speed was low when compared with $H=0.1m$ this is on the grounds that in the procedures of bed expanded from the 0.1m to 0.22m due to the kinetic energy was lost by the particles.



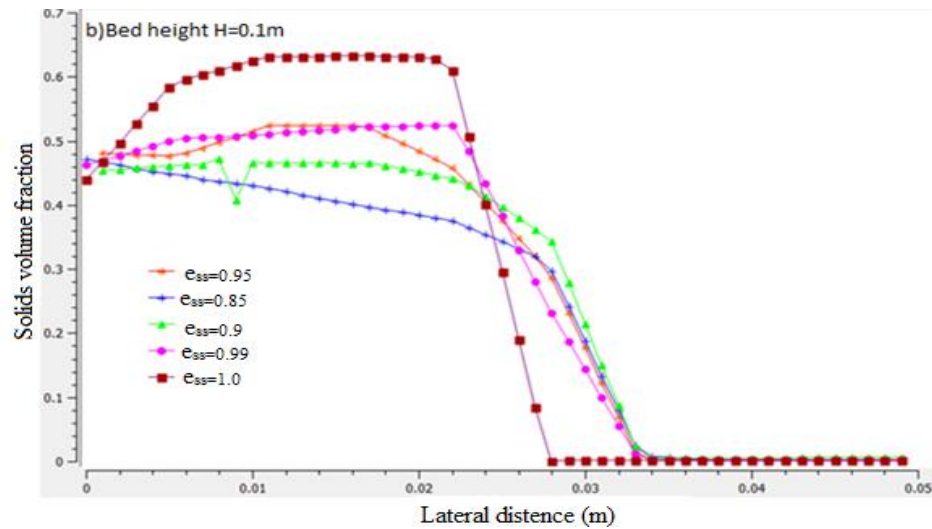
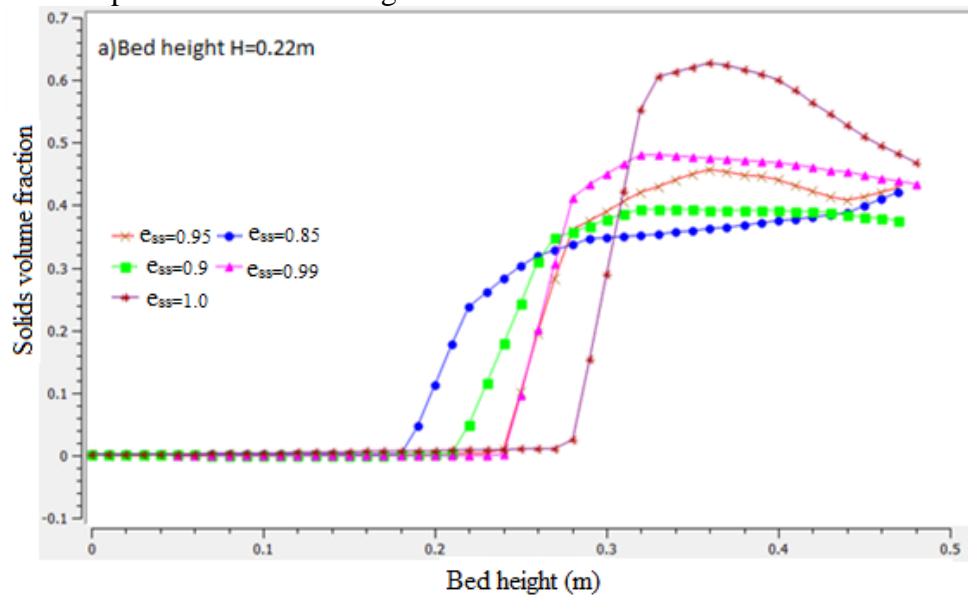


Fig.6 Time-averaged volume fraction profiles of solids along the lateral direction for varies coefficient of restitutions at different bed heights a)0.22 m and b)0.1m

From fig 6. The solids volume fraction was varied at different restitution coefficients and at different bed heights by increasing the interactions between the solids, so they were gain the much of kinetic energy and that solids volume fraction along the lateral distance was high, and also from the bed height to bed height the lateral distance was changed at bed height H=0.22m and it was low when compare to lower bed height H=0.1m.



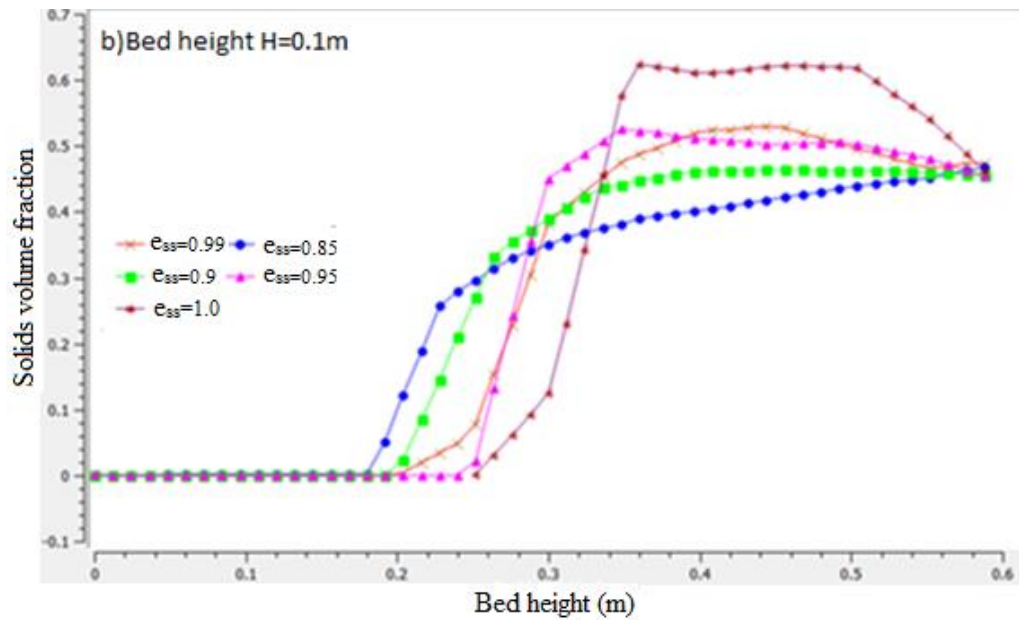
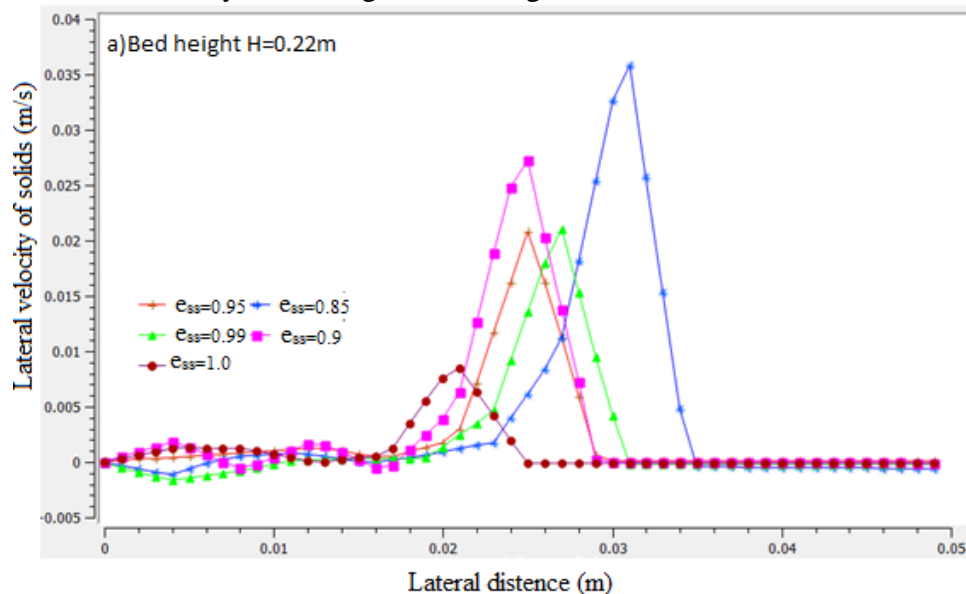


Fig .7 Axial trends of time-averaged solids volume fractions for varies coefficient of restitutions at varies bed heights a)0.22 m and b)0.1m

From the fig 7,the axial velocity of solid particle profiles along the lateral direction at different restitution coefficients 1.0, 0.99, 0.95, 0.90 and 0.85 respectively and also by changing bed heights (0.22m and 0.1m) from the outlet. The lateral velocity of the solid phase along the lateral distance increased by increasing the interaction between the solids (at restitution coefficient 1.0 and 0.99) and at remaining restitution coefficients the velocity almost same there is no effect. The negative velocity referred that it is in negative hand side of the imaginary axis and positive velocity referred that it is in the right-hand side of the imaginary axis. And it was observed that the solids were carried down from the top by the inlet flow velocity of water. When compare the bed heights along the fluidized bed the lateral velocity along the lateral distance will be increased by increasing the bed heights.



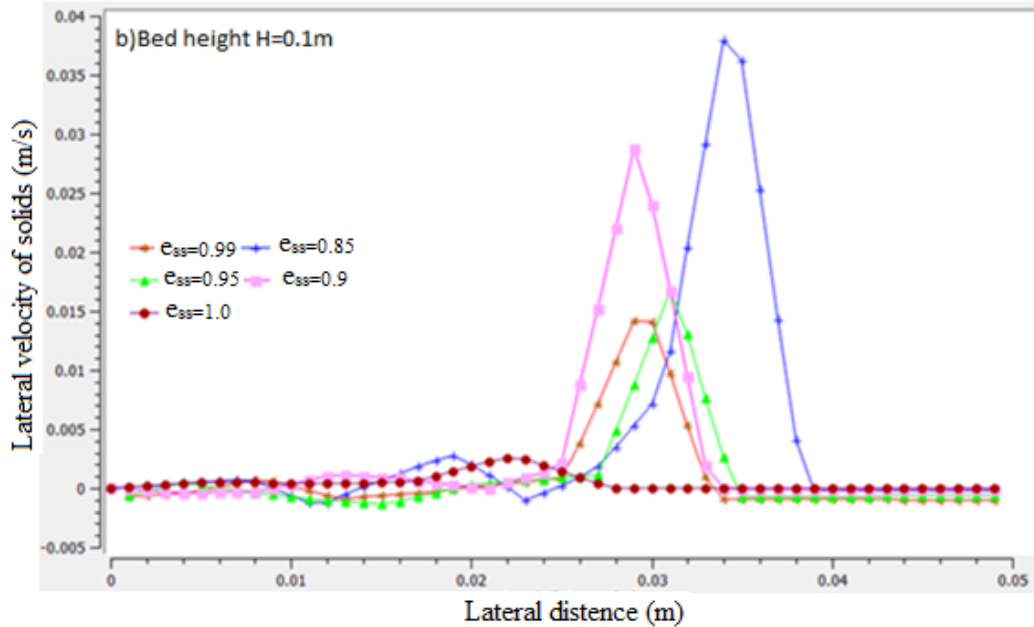
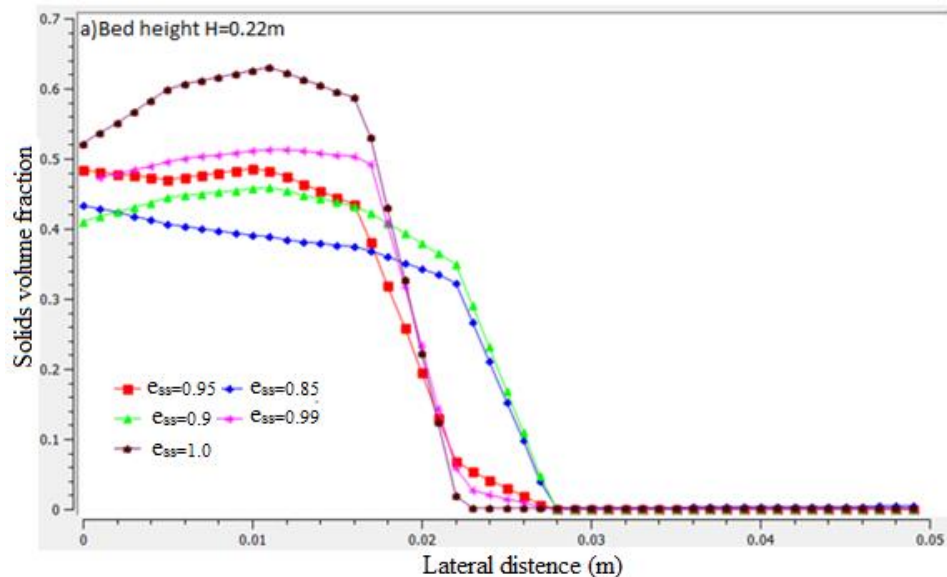


Fig .8 lateral velocity profiles of solids along the lateral direction for various coefficient restitution at different bed heights a)0.22 m and b)0.1m

From the Fig.8 lateral velocity profiles along lateral distance was increased at middle point region of the bed almost zero velocity at walls of the bed by increasing the restitution coefficient at $e_{ss}=0.99$ and $e_{ss}=0.9$ and at remaining the velocity was almost the same, and when compare to specularity coefficient ($\phi = 1.0$) in this the velocity profile was less why because at ($\phi = 0.5$) the interaction between the solid-wall less so velocity was also less.



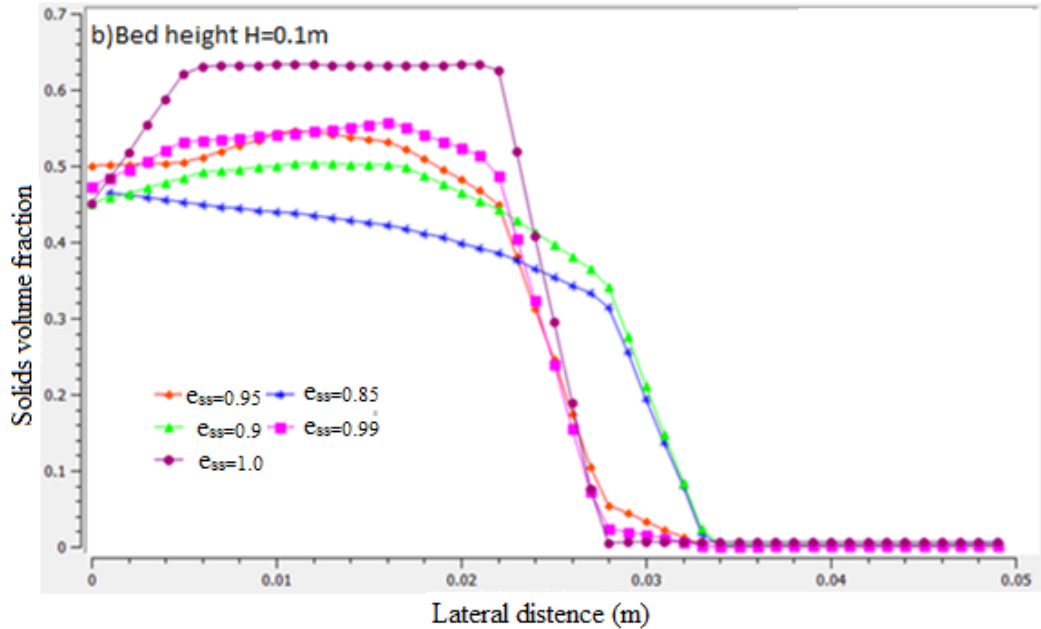
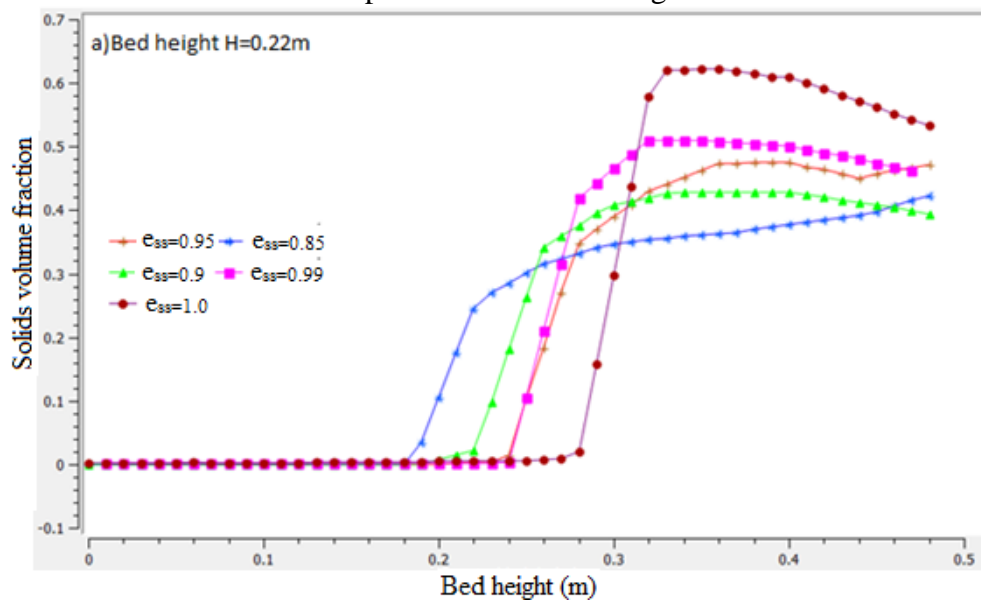


Fig.9 Time-averaged solids volume fraction profiles along the lateral direction of the bed for varies coefficient of restitutions at different bed heights a)0.22 m and b)0.1m

From fig 9The particles volume fraction was varied at different restitution coefficients and at extraordinary bed heights by increasing the interactions between the solid, so they were gain the much kinetic energy and that solids volume fraction along the lateral distance was almost the same and also from the bed height to bed height the lateral distance was changed at bed height $H=0.22m$ was low when compared to lower bed height $H=0.1m$.



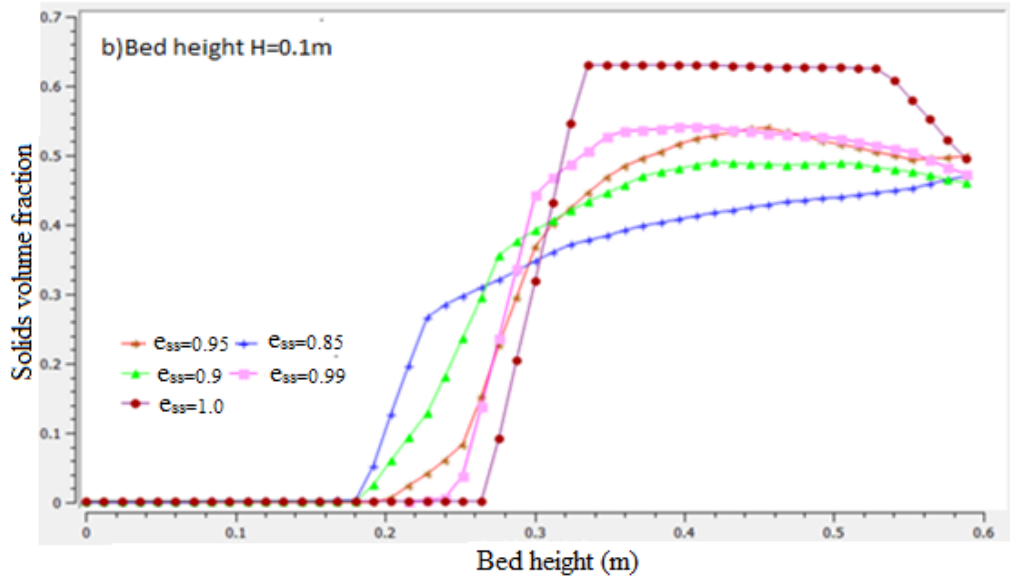


Fig .10 Time-averaged solids volume fraction profiles along the axial direction of the bed for varies coefficient of restitutions at different bed heights a)0.22 m and b)0.1m

From the fig 10, the axial Volume fraction trends of solids along the reactor heights at varies restitution coefficients 1.0, 0.99, 0.95, 0.9 and 0.85 respectively and also by changing bed heights(0.22m and 0.1m) from the outlet. The volume fraction of solids along the pivotal distance increased by increasing the interaction between the particles (at restitution coefficient 0.99 and 1.0) and at remaining restitution coefficients the volume fraction almost had the little bit of effect.

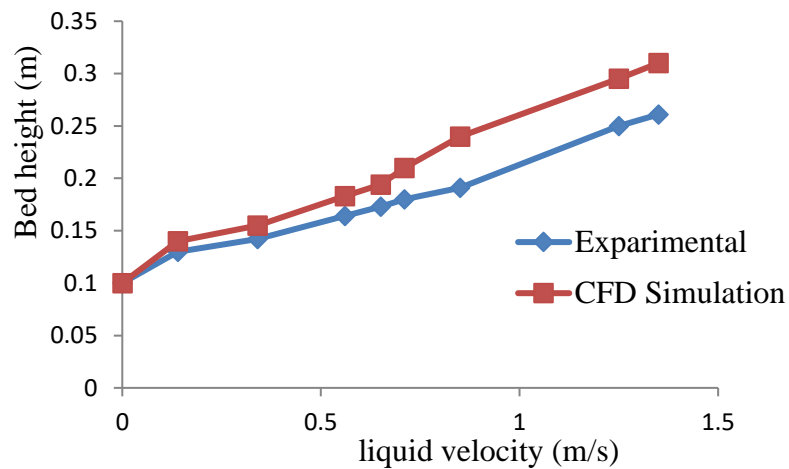


Fig .11 Simulated Bed expansion profiles comparison with experimental data for solids at different velocities

From the Fig 11. We observed that by increasing the velocity the bed was expanded these were we compared by experimental results with simulated results from that almost trend was same and also from the fig 12 the Voidage was increased by increasing the velocity the trend was same when compare

experimental results with simulated results. When observed the present work (inverse solid-liquid fluidization) bed expansion profiles with similar previous works [17] in mc group the bed was expanded by increasing the up-flow velocity range (14.6-26.77)mm/s , density of solids is (1600-1687) kg/m³, initial volume fraction used in the simulation is(0.099-0.102)and initial bed height is 216mm it is increased to 500mm,in the present tapered inverse solid-liquid inverse fluidization the downflow liquid velocity is (0.14-0.135) m/s, density of solids is 895 kg/m³,initial bed height is 0.1m,initial volume fraction used in the simulation is 0.6 and that bed is expanded to 0.26m.In the both previous work and in the inverse fluidization bed expansion profiles were same but in the present work the flow requirement is less. By observed similar earlier work[11].

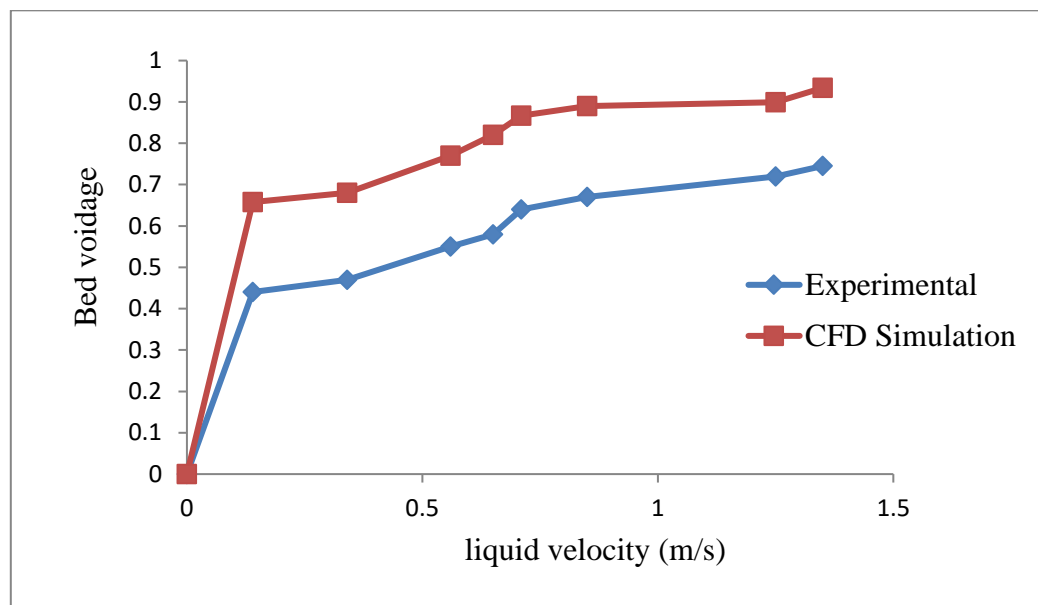


Fig .12 Comparison of simulated Voidage profiles with experimental data for solids at different velocities

5. Conclusions

By changing the restitution coefficient(0.85,0.9,0.95 and1.0)between the solid-solid and specularity coefficient (0.5, 1.0) interaction between the solid-wall there was a lot of effect on the behavior of hydrodynamics of inverse fluidized bed. At different restitution coefficients, there was dissimilar results of solid volume fraction along lateral distance and axial distance and lateral velocity of particles along the lateral distance of different bed heights. We found that the most of the effect is at $\text{ess}=0.99$ and 0.95 due to that at this interaction, collisions between them very high and elaborated kinetic energy between them and we get desired results when compared other restitution coefficients. And bed height, Voidage profiles by simulated results and experimental results almost the same.

Funding:

This research received no external funding

Conflicts of Interest:

The author declares no conflict of interest

References

- Kumar U, Agarwal VK . Simulation of 3D gas-solid fluidized bed reactor hydrodynamics. *Part Sci Technol.*2017, 35, 1–13 .
- Wang S, Sun J, Yang Q, et al. Numerical simulation of flow behavior of particles in an inverse liquid-solid fluidized bed. *Powder Technol.* 2014. 261, 14–21 04.017
- Ulaganathan N, Krishnaiah K. Hydrodynamic characteristics of two-phase inverse fluidized bed. *Bioprocess Eng.*1996,15,159–164 .
- Campos-Díaz KE, Bandala-González ER, Limas-Ballesteros R . Fluid bed porosity mathematical model for an inverse fluidized bed bioreactor with particles growing biofilm. *J Environ Manage.* 2012, 104,62–66 .
- Renganathan T, Krishnaiah K . Prediction of Minimum Fluidization Velocity in Two and Three Phase Inverse Fluidized Beds. *Can J Chem Eng.*2003, 81,853–860 .
- Arun N, Razack AA, Sivasubramanian V .Recent Progress in Hydrodynamics of Inverse Fluidized Bed Reactors: a Review. *Chem Eng Commun.*2013, 200,1260–1277 .
- Cornelissen JT, Taghipour F, Escudié R, et al. CFD modelling of a liquid-solid fluidized bed. *Chem Eng Sci.*2007, 62,6334–6348 .
- Sur DH, Mukhopadhyay M . Process aspects of three-phase inverse fluidized bed bioreactor: A review. *J Environ Chem Eng.*2017, 5,3518–3528 .
- Hamdad I, Hashemi S, Rossi D, Macchi A. Oxygen transfer and hydrodynamics in three-phase inverse fluidized beds. *Chem Eng Sci.*2007, 62,7399–7405 .
- Lakshmi ACV, Balamurugan M, Sivakumar M, et al. Minimum fluidization velocity and friction factor in a liquid-solid inverse fluidized bed reactor. *Bioprocess Eng.*2009, 22,461–466 .
- Jack T. Cornelissen, Fariborz Taghipour, Renaud Escudié, Naoko Ellis, John R. Grace, et al. CFD modeling of a liquid-solid fluidized bed. *Chem Eng Sci.*2007,62, 6334 – 6348.
- D.C. Sau, K.C. Biswal, et al .Computational fluid dynamics and experimental study Of the hydrodynamics of a gas-solid tapered fluidized bed. *Applied Mathematical Modeling.*2009, 35, 2265–2278
- Shujun Geng, Yanan Qian, Jinhui Zhan, Hongling Zhang, Guangwen Xu, Xiaoxing Liu et al. Prediction of solids residence time distribution in cross-flow bubbling fluidized bed. *Powder Technology.*2017,320,555–564.
- Y.J. Liu, X.Y. Lan, C.M. Xu, G. Wang, J.S. Gao, et al. CFD simulation of gas and solids mixing in FCC strippers, *AIChE J.*2012, 58, 1119–1132.

- Rupesh K. Reddy, Jyeshtharaj B. Joshi, et al. CFD modeling of solid-liquid fluidized beds of mono and binary particle mixtures, *Chem Eng Sci.*2009, 64,3641 – 3658.
- Mikele Cândida Sousa Sant'Anna, Wenna Raissa dos Santos Cruz, Gabriel Francisco da Silva, Ricardo de Andrade Medronho, Sergio Lucena, et al. Analyzing the fluidization of a gas-sand-biomass mixture using CFD techniques, *Powder Technology.*2017,316,367–372.
- Md. Saifur Rahaman, Mahbuboor R. Choudhury, Amruthur S. Ramamurthy, Donald S. Mavinic, Naoko Ellis, Fariborz Taghipour, et al. CFD modeling of liquid-solid fluidized beds of polydisperse struvite crystals, *International Journal of Multiphase Flow.*2018, 99,48–61.
- Dinesh V. Kalaga, Rupesh K. Reddy, Jyeshtharaj B. Joshi, Sameer V. Dalvi, K. Nandkumar, et al. Liquid phase axial mixing in solid-liquid circulating multistage fluidized bed: CFD modeling and RTD measurements, *Chem Eng Journal.*2012, 191,475– 490.
- Maryam Askarishahi, Mohammad-Sadegh Salehi, Hamid Reza Godini, GünterWozny,et al .CFD study on solids flow pattern and solids mixing characteristics bubbling Fluidized bed: Effect of fluidization velocity and bed aspect ratio,*Powder Technology* .2015,274,379–392